

N85-31210

# COMBINED STATE AND PARAMETER ESTIMATION FOR A STATIC MODEL OF THE MAYPOLE (HOOP/COLUMN) ANTENNA SURFACE

**H. T. Banks**

Lefschetz Center for Dynamical Systems  
Brown University  
Providence, RI 02912

**P. K. Lamm**

Southern Methodist University  
Dallas, TX 75275

**E. S. Armstrong**

NASA Langley Research Center  
Hampton, VA 23665

## ABSTRACT

Parameter and state estimation techniques are discussed for an elliptic system arising in a developmental model for the antenna surface of the Maypole Hoop/Column antenna. A computational algorithm based on spline approximations for the state and elastic parameters is given and numerical results obtained using this algorithm are summarized.

## I. INTRODUCTION

Results are presented from a Langley program directed towards developing computationally efficient identification techniques for flexible systems modeled by partial differential equations with an emphasis on large space structures. Initial efforts have been directed towards extending the spline-based theory and computational techniques used by the first two authors [1]-[6] in solving identification problems with delay and partial differential equation models in one spatial variable to solve distributed problems in several spatial variables. Additionally, in order to support Langley's technology development program [7] in large space antennae, a parameter and state estimation algorithm has been derived for a prototype distributed model of the Maypole (Hoop/Column) antenna reflector surface [8]. The next section describes the Hoop/Column antenna and presents the identification problem being considered. The state and parameter estimation approach is then outlined and discussed in the context of the Hoop/Column application. Subsequent sections include mathematical details of the antenna application and numerical results.

PRECEDING PAGE BLANK NOT FILMED

## II. THE MAYPOLE (HOOP/COLUMN) ANTENNA

For the purpose of technology development, the NASA Large Space Systems Technology (LSST) program office has pinpointed focus missions and identified future requirements for large space antennas for communications, earth sensing, and radio astronomy [7]. In this study, particular emphasis is placed on mesh deployable antennas in the 50-120 meter diameter category. One such antenna is the Maypole (Hoop/Column) antenna shown for the 100m point-design in Figures 1 and 2. This antenna concept is being developed by the Harris Corporation, Melbourne, Florida, under contract to the Langley Research Center [8].

The Hoop/Column antenna consists of a knitted gold-plated molybdenum wire reflective mesh stretched over a collapsible hoop that supplies the rigidity necessary to maintain a circular outer shape. The annular membrane-like reflector surface surrounds a telescoping mast which provides anchoring locations for the mesh center section (Fig. 1). The mast also provides anchoring for cables that connect the top end of the mast to the outer hoop and the bottom end of the mast to 48 equally spaced radial graphite cord truss systems woven through the mesh surface [8]. Tensions on the upper (quartz) cables and outer lower (graphite epoxy) cables are counter balanced to provide stiffness to the hoop structure. The inner lower cables produce, through the truss systems, distributed surface loading to control the shape of four circular reflective dishes (Figs. 1 and 2) on the mesh surface.

After deployment or after a long period of operation, the reflector surface may require adjustment. Optical sensors are to be located on the upper mast which measure angles of retroreflective targets placed on the truss radial cord edges on the antenna surface. This information can then be processed using a ground-based computer to determine a data set of values of mesh surface location at selected target points. If necessary, a new set of shaping (control) cord tensions can be fed back to the antenna for adjustment.

It is desirable to have an identification procedure which allows one to estimate the antenna mesh shape at arbitrary surface points and the distributed loading from data set observations. It can also be anticipated that environmental stresses and the effects of aging will alter the mesh material properties. The identification procedure must also allow one to address this issue.

Considering the antenna to be fully deployed and in static equilibrium, a distributed mathematical model which describes the antenna surface deviation from a curved equilibrium configuration is under investigation (for preliminary findings, see [9]). Using a cylindrical coordinate system with the z-axis along the mast, it is expected that the resulting model will entail a system of coupled second-order linear partial differential

equations in two spatial variables. The coefficients of these equations are functions of the material properties of the stretched mesh. The derivation and computer software for this model are still under development. In the meantime, a simpler developmental (prototype) problem has been solved which is descriptive of the original problem.

For the developmental problem, the loading is assumed to be normal to the horizontal plane containing the hoop rim, and the mesh surface is assumed to be described by the static two-dimensional stretched membrane equation [10] with variable stiffness (elastic) coefficients and appropriate boundary conditions for the Hoop/Column geometry. Mathematically, in polar coordinates, we have

$$-\frac{1}{r} \frac{\partial}{\partial r} \left[ rE(r, \theta) \frac{\partial u}{\partial r} \right] - \frac{1}{r^2} \frac{\partial}{\partial \theta} \left[ E(r, \theta) \frac{\partial u}{\partial \theta} \right] = f(r, \theta) \quad (1)$$

where  $u(r, \theta)$  is the vertical displacement of the mesh from the hoop plane,  $f(r, \theta)$  is the distributed loading force per unit area, and  $E(r, \theta) > 0$  is the distributed stiffness (elastic) coefficient of the mesh surface (force/unit length). Equation (1) is to be solved over the annular region  $\Omega = [\epsilon, R] \times [0, 2\pi]$ . Appropriate boundary conditions are

$$\begin{aligned} u(\epsilon, \theta) &= u_0 \\ u(R, \theta) &= 0 \end{aligned} \quad (2)$$

along with the periodicity requirement

$$u(r, 0) = u(r, 2\pi), \quad (3)$$

where  $R$  is the radius from the mast center to the circular outer hoop,  $\epsilon$  is the radius from the mast to the beginning of the mesh surface (see Fig. 2), and  $u_0$  is the coordinate at  $r = \epsilon$  of the mesh surface below the outer hoop plane.

We further assume that the distributed loading along with a data set of vertical displacements,  $u_m(r_i, \theta_j)$ , at selected points  $(r_i, \theta_j)$  on the mesh surface is known. Given this information, the developmental problem is to estimate the material properties of the mesh as represented by  $E(r, \theta)$  and produce state estimates of the surface represented by  $u(r, \theta)$  at arbitrary  $(r, \theta)$  points within  $\Omega$ . The procedure applied to solve this problem is discussed in the next section.

### III. THE SYSTEM IDENTIFICATION APPROACH

The first two authors and their colleagues have derived techniques for approximating the solutions to systems identification and control problems involving delay equation models and partial differential equation models in one spatial variable and have used them in a variety of applications [11],[12]. The Hoop/Column application requires an extension of the theory and numerical algorithms to elliptic distributed systems in several spatial variables. The approach, when specialized to the system identification problem, may be summarized as follows: (1) select a distributed parameter formulation containing unknown parameters for a specific system; (2) mathematically "project" the formulation down onto a finite dimensional subspace through some approximation procedure such as finite differences, finite elements, etc.; (3) solve the identification problem within the finite dimensional subspace obtaining an estimate dependent upon the order of the approximation embodied in the subspace; (4) successively increase the order of the approximation and, in each case, solve the identification problem so as to construct a sequence of parameter and state estimates ordered with increasing refinement of the approximation scheme; (5) seek a mathematical theory which provides conditions under which the sequence of approximate solutions approaches the distributed solution as the subspace dimension increases with a convergent underlying sequence of parameter estimates.

In applying this approach to the developmental problem, the stiffness function is parametrized in terms of cubic splines of fixed order; this converts the estimation of  $E(r,\theta)$  into a finite dimensional parameter estimation problem. After writing the energy functional generic to the membrane equation, the Galerkin procedure is used to project the distributed formulation onto a finite dimensional state subspace spanned by tensor products of linear spline functions defined over  $\Omega$ . The approximate displacement (state estimate) thus obtained is expressible in terms of the spline basis functions. The Galerkin procedure in this case yields algebraic equations which define the displacement approximation coordinates in terms of the unknown  $E(r,\theta)$  parameters. In order to solve the approximating parameter estimation problem, the parameters defining  $E(r,\theta)$  are chosen so that a least squares measure of the fit error between the observed and predicted (by the estimated state) data set is minimized. Finally, following steps (4) and (5) an algorithm is constructed to determine the order of the linear spline approximation above which little or no further improvement is obtained in the unknown quantities as one increases the dimension of the subspaces. Details of this system identification approach are presented in the following sections.

#### IV. FINITE DIMENSIONAL APPROXIMATIONS

Prior to applying the Galerkin procedure [13,14] to perform the finite dimensional approximation for the developmental problem, the boundary conditions (2) are converted to homogeneous form by introducing the new dependent variable

$$y(r,\theta) = u(r,\theta) - \left(\frac{r-R}{\epsilon-R}\right) u_0 \quad (4)$$

Equation (1) then becomes

$$-\frac{1}{r} \frac{\partial}{\partial r} \left( r E(r,\theta) \frac{\partial y}{\partial r} \right) - \frac{1}{r^2} \frac{\partial}{\partial \theta} \left( E(r,\theta) \frac{\partial y}{\partial \theta} \right) = f(r,\theta) + \frac{1}{r} \frac{\partial}{\partial r} \left( \frac{r E(r,\theta) u_0}{\epsilon - R} \right) \quad (5)$$

with boundary conditions

$$\begin{aligned} y(\epsilon,\theta) &= 0 \\ y(R,\theta) &= 0 \\ y(r,0) &= y(r,2\pi) . \end{aligned} \quad (6)$$

Following the standard formulation (see [13,14]) for the weak or variational form of (5), the energy functional  $\hat{E}$  associated with (5) is

$$\hat{E}(z) = \int_0^{2\pi} \int_r^R \left[ \frac{1}{2} E(r,\theta) \nabla z \cdot \nabla z - f(r,\theta) z \right] r dr d\theta , \quad (7)$$

where  $\nabla$  is the gradient in polar coordinates which, in the form used here, is equivalent to

$$\left( \frac{\partial}{\partial r} , \frac{1}{r} \frac{\partial}{\partial \theta} \right)^T . \quad (8)$$

The function  $\tilde{f}$  is given by

$$\tilde{f}(r,\theta) = f(r,\theta) + \frac{1}{r} \frac{\partial}{\partial r} \left( \frac{r E(r,\theta) u_0}{\epsilon - R} \right) \quad (9)$$

and the vertical displacement  $z(r,\theta)$  of the mesh surface away from the hoop equilibrium plane is a function satisfying the boundary conditions (6) and possessing first derivatives on  $\Omega$  in the distributional sense (we denote this by  $z \in H_{0,per}^1(\Omega) \equiv Z$ ). The first variation  $\delta \hat{E}$  of  $\hat{E}$  about the function  $y(r,\theta)$  is given by

$$\begin{aligned} \hat{\delta E}(y; v) &= \int_0^{2\pi} \int_{\epsilon}^R \{E(r, \theta) \nabla y \cdot \nabla v - \tilde{f}(r, \theta) v\} r dr d\theta \\ &= \int_0^{2\pi} \int_{\epsilon}^R \{E(r, \theta) \nabla y \cdot \nabla v - [f(r, \theta) v + E(r, \theta) \tilde{k} \cdot \nabla v]\} r dr d\theta \end{aligned} \quad (10)$$

where

$$\tilde{k} = \begin{pmatrix} k \\ 0 \end{pmatrix} = \begin{pmatrix} \frac{u_0}{R-\epsilon} \\ 0 \end{pmatrix} \quad (11)$$

and  $v$  is an arbitrary function in  $Z = H_{0, \text{per}}^1(\Omega)$ .

Given a finite dimensional subspace  $\hat{Z}$  of  $Z$ , the Galerkin procedure defines the approximation  $\hat{y}$  as the solution in  $\hat{Z}$  of

$$\int_0^{2\pi} \int_{\epsilon}^R \{E(r, \theta) \hat{\nabla} y \cdot \hat{\nabla} v\} r dr d\theta = \int_0^{2\pi} \int_{\epsilon}^R \{f(r, \theta) \hat{v} + E(r, \theta) \tilde{k} \cdot \hat{\nabla} v\} r dr d\theta \quad (12)$$

for all  $\hat{v} \in \hat{Z}$ .

For computational efficiency, the basis functions used for the representations of  $\hat{y}$  in (12) are taken as tensor products of linear B-splines ([13], p. 27; [14], p. 100). Thus  $\hat{v}$  and  $\hat{y}$  are in the space spanned by

$$v_{ij}^{M,N}(r, \theta) = \alpha_i^M(r) \beta_j^N(\theta), \quad (i = 1, \dots, M-1; j = 1, \dots, N), \quad (13)$$

where  $\alpha_i^M = \alpha_i^M(r)$ , ( $i = 1, \dots, M-1$ ), and  $\beta_j^N = \beta_j^N(\theta)$ , ( $j = 1, \dots, N-1$ ), are standard linear B-splines with knots uniformly spaced over  $[\epsilon, R]$  and  $[0, 2\pi]$ , respectively, modified to satisfy the appropriate boundary conditions. The elements  $\{\alpha_i^M\}$  are modified to satisfy homogeneous boundary conditions while  $\beta_N^N$  has been altered to satisfy periodic boundary conditions [15].

For  $y^{M,N}(r,\theta)$  within the subspace spanned by  $v_{ij}^{M,N}$  we can write

$$y^{M,N}(r,\theta) = \sum_{i=1}^{M-1} \sum_{j=1}^N \alpha_i^M(r) w_{ij}^{M,N} \beta_j^N(\theta) . \quad (14)$$

Replacing  $\hat{y}(r,\theta)$  in (12) by  $y^{M,N}(r,\theta)$  from (14) and successively setting  $v(r,\theta) = v_{ij}^{M,N}(r,\theta)$  for  $i = 1, \dots, M-1$  and  $j = 1, \dots, N$  leads to a set of high-order linear algebraic equations for the  $w_{ij}^{M,N}$  coordinates.

We avoid sparse matrix methods in solving the  $w_{ij}^{M,N}$  equation by imposing a separability condition:

$$E(r,\theta) = E_1(r)E_2(\theta) . \quad (15)$$

As shown in [15], condition (15) reduces the  $w_{ij}^{M,N}$  calculation to the solution of the matrix equation

$$\tilde{B}^M W^{M,N} \tilde{A}^N + \tilde{D}^M W^{M,N} \tilde{C}^N = \tilde{E}^{M,N} \quad (16)$$

with

$$W^{M,N} = \left( w_{ij}^{M,N} \right) \quad (17)$$

$$\tilde{A}^N = \left( \int_C^{2\pi} E_2(\theta) \beta_j^N(\theta) \beta_q^N(\theta) d\theta \right) \quad (18)$$

$$\tilde{B}^M = \left( \int_\epsilon^R E_1(r) \left[ \frac{d}{dr} \alpha_i^M(r) \right] \left[ \frac{d}{dr} \alpha_p^M(r) \right] r dr \right) \quad (19)$$

$$\tilde{C}^N = \left( \int_0^{2\pi} E_2(\theta) \left[ \frac{d}{d\theta} \beta_j^N(\theta) \right] \left[ \frac{d}{d\theta} \beta_q^N(\theta) \right] d\theta \right) \quad (20)$$

$$\tilde{D}^M = \left( \int_\epsilon^R E_1(r) \frac{\alpha_i^M(r) \alpha_p^M(r)}{r} dr \right) \quad (21)$$

and

$$\begin{aligned} \tilde{c}^{M,N} = & \left( \int_0^{2\pi} \int_{\epsilon}^R f(r,\theta) \alpha_1^M(r) \beta_j^N(\theta) r dr d\theta \right. \\ & \left. + \int_0^{2\pi} \int_{\epsilon}^R E(r,\theta) \hat{k} \beta_j^N(\theta) \left[ \frac{d}{dr} \alpha_1^M(r) \right] r dr d\theta \right), \end{aligned} \quad (22)$$

where, in (17)-(22),  $i, p = 1, \dots, M-1$  and  $j, q = 1, \dots, N$ .

Equation (16) is rewritten in the equivalent form

$$\left[ (\tilde{D}^M)^{-1} \tilde{B}^M \right] W^{M,N} + W^{M,N} \left[ \tilde{C}^N (\tilde{A}^N)^{-1} \right] = (\tilde{D}^M)^{-1} \tilde{E}^{M,N} (\tilde{A}^N)^{-1} \quad (23)$$

and solved by the Bartels-Stewart algorithm [16].

In order to estimate, via a numerical scheme, the functional coefficients  $E_1$  and  $E_2$ , we parametrize these functions so that identification is performed over a finite-dimensional parameter set. To this end, let

$$E_1(r) = \sum_{k=1}^{M_1} v_k \lambda_k(r) \quad (24)$$

$$E_2(\theta) = \sum_{j=1}^{N_1} \delta_j \mu_j(\theta) \quad (25)$$

where  $v_k$  and  $\delta_j$  are scalar parameters and  $\lambda_k$  and  $\mu_j$  are cubic B-spline functions defined [13, p. 61] over  $[\epsilon, R]$  and  $[0, 2\pi]$ , respectively, whose orders are independent of  $M$  and  $N$ . The basic spline functions are modified so that  $\mu_j$  and its derivatives satisfy periodic boundary conditions.

We turn next to the computer implementation of the identification scheme.



## V. COMPUTATIONAL PROCEDURE

Appealing to the ideas found in previous sections, we now detail an algorithm for estimating the coefficients  $v_k$ ,  $k = 1, \dots, M_1$  and  $\delta_j$ ,  $j = 1, \dots, N_1$ , for  $E(r, \theta)$  that provide the "best fit" between estimations of the state  $u$  and observed data  $u_m$  obtained from various sample points on the surface. We may equivalently consider data for  $y$  by making the transformation

$$y_m(r_i, \theta_j) = u_m(r_i, \theta_j) - \left( \frac{r_i - R}{\varepsilon - R} \right) u_0 \quad (26)$$

for  $i = 1, \dots, L_r$  and  $j = 1, \dots, L_\theta$ .

A parameter estimation algorithm may be organized into the following steps.

1. Select an order of approximation for the cubic spline elements  $\lambda_k$ ,  $k = 1, \dots, M_1$  and  $\mu_j$ ,  $j = 1, \dots, N_1$ , used to represent  $E_1$  and  $E_2$ . Set  $n = 1$ .
2. Select  $M$  and  $N$ , the number of the linear spline basis elements used to represent  $u^{M,N}$  (and  $y^{M,N}$ ).
3. Assume a nominal set of values for

$$v = (v_1, v_2, \dots, v_{M_1}) \quad (27)$$

and

$$\delta = (\delta_1, \delta_2, \dots, \delta_{N_1}) . \quad (28)$$

4. Calculate the coefficient matrices in (23) and solve for  $w^{M,N}(v, \delta)$ .
5. Calculate, from (14),  $y^{M,N}(r_i, \theta_j; v, \delta)$  and evaluate

$$J^{M,N}(v, \delta) = \sum_{i=1}^{L_r} \sum_{j=1}^{L_\theta} \left[ y^{M,N}(r_i, \theta_j; v, \delta) - y_m(r_i, \theta_j) \right]^2 . \quad (29)$$

6. Proceed to step 8 if  $J^{M,N}(v, \delta)$  is sufficiently small. Otherwise, through an optimization procedure, determine a new pair  $(\hat{v}, \hat{\delta})$  which decreases the value of  $J^{M,N}$ . If no such pair can be found, go to step 8.

7. Set  $(\nu, \delta) = (\hat{\nu}, \hat{\delta})$  and return to step 4.
8. Preserve the current values of  $y^{M,N}$  and the corresponding  $(\nu, \delta)$  pair as the  $n^{\text{th}}$  entry in a sequence of these pairs, ordered with increasing  $M$  and  $N$ .
9. Proceed to step 10 if sufficient data has been obtained to analyze the sequences. Otherwise, set  $n = n + 1$  and return to step 2 with increased  $M$  and  $N$ . The current values of  $(\nu, \delta)$  will be used as initial values for the next optimization process.
10. From analysis of the numerical sequences, select the  $(M,N)$  entry which indicates the best numerical results. The corresponding parameter estimate  $(\nu, \delta)$  pair yields  $E(r, \theta)$  which determines the material properties of the antenna mesh. The matrix  $w^{M,N}(\nu, \delta)$ , when used in conjunction with (14), determines a state approximation  $y^{M,N}$  for the shape of the antenna surface.

A convergence theory for the identification algorithm may be found in [15]. Numerical results are described in the next section.

## VI. NUMERICAL RESULTS

Experimental data for the Hoop/Column antenna is not available at this time. Therefore, synthetic data is constructed to demonstrate the preceding algorithm.

As shown in Figure 2, the parent reflector has four separate areas of illumination on its surface. Each area is assumed to have the same parabolic shape. For  $0 \leq \theta \leq \frac{\pi}{2}$  and  $\epsilon \leq r \leq R$ .

$$u^0(r, \theta) = \begin{cases} \frac{u_0(R - r)}{R - \epsilon} \left[ k \left( \frac{r - \epsilon}{R} \right) q_2(\theta) + 1 \right], & 0 \leq \theta \leq \frac{\pi}{36} \\ \frac{u_0(R - r)}{R - \epsilon} \left[ k \left( \frac{r - \epsilon}{R} \right) q_1(\theta) + 1 \right], & \frac{\pi}{36} \leq \theta \leq \frac{17\pi}{36} \\ \frac{u_0(R - r)}{R - \epsilon} \left[ k \left( \frac{r - \epsilon}{R} \right) q_3(\theta) + 1 \right], & \frac{17\pi}{36} \leq \theta \leq \frac{\pi}{2} \end{cases} \quad (30)$$

where

$$q_1(\theta) = \sin\theta + \cos\theta . \quad (31)$$

The functions  $q_2(\theta)$  and  $q_3(\theta)$  are cubic polynomial fits used to ensure smoothness in regions of  $\theta$  near  $\theta = \frac{\pi}{2}, \pi, \frac{3\pi}{2}, 2\pi$ . Formulae for  $q_2(\theta)$  and  $q_3(\theta)$  may be found in [15]. The parameter  $k > 0$ , a stretch factor used to perturb the surface below the conic ( $k = 0$ ) shape is taken as 0.25.

For the complete surface, we define, for  $\epsilon \leq r \leq R$ ,

$$\bar{u}(r, \theta) = \begin{cases} u^0(r, \theta) , & 0 \leq \theta \leq \frac{\pi}{2} \\ u^0\left(r, \theta - \frac{\pi}{2}\right) , & \frac{\pi}{2} \leq \theta \leq \pi \\ u^0(r, \theta - \pi) , & \pi \leq \theta \leq \frac{3\pi}{2} \\ u^0\left(r, \theta - \frac{3\pi}{2}\right) , & \frac{3\pi}{2} \leq \theta \leq 2\pi . \end{cases} \quad (32)$$

It is expected that the mesh will be stiffest near the outer hoop ( $r = R$ ) and around the inner radius ( $r = \epsilon$ ). For this reason we choose a known value of  $E_1(r)$  as

$$\bar{E}_1(r) = 2\hat{\tau} - \hat{\tau} \sin \left[ \pi \frac{(r - \epsilon)}{(R - \epsilon)} \right] \quad (\epsilon \leq r \leq R) \quad (33)$$

where  $\hat{\tau}$  is a constant dependent on the mesh material. The stiffness in the angular direction is expected to be uniform with

$$\bar{E}_2(\theta) \equiv \hat{\tau} . \quad (34)$$

From data provided [8] for the 10<sup>7</sup>-meter point design, a reasonable value for  $\hat{\tau}$  (given in units  $\sqrt{N/m}$ ) is

$$\hat{\tau} = 3.391 ; \quad (35)$$

similarly, other parameters are calculated to be  $u_0 = -7.5m$ ,  $\epsilon = 8.235m$  and  $R = 50m$ .

A 10 x 24 grid of data points  $u_m(r_i, \theta_j)$  is calculated by evaluating  $\bar{u}(r, \theta)$  at points  $(r_i, \theta_j)$  with

$$r_i = \epsilon + i \frac{(R - \epsilon)}{L_r} \quad (i = 1, 2, \dots, L_r = 10) \quad (36)$$

$$\theta_j = [7.5^\circ + (j - 1) 15^\circ] \frac{\pi}{180} \quad (j = 1, 2, \dots, L_\theta = 24) \quad (37)$$

Values of  $\theta_j$  correspond to data taken along every other radial cord truss system with reflectors assumed located on the gore edges. Distributed loads are obtained by substituting (32)-(34) into (1) and evaluating  $f(r, \theta)$ .

In the examples of the identification process to be presented, an equal number of linear spline basis functions are used in both  $r$  and  $\theta$  directions. That is,  $M = N + 1$  for an increasing sequence of  $N$ -values. The cubic spline approximations (24) and (25) are used with fixed  $M_1 = N_1 = 4$  to represent  $E_1(r)$  and  $E_2(\theta)$ . The IMSL version (ZXSSQ) of the Levenberg-Marquardt algorithm [17] is employed to minimize  $J^{M,N}$  given by (29). For the first choice of  $N$ , nominal  $(v, \delta)$  parameter values to initialize the Levenberg-Marquardt algorithm are obtained by finding those  $(v, \delta)$  coordinates which cause (24) and (25) to best approximate assumed functions  $E_1^0(r)$  and  $E_2^0(\theta)$  chosen as guessed forms for  $\bar{E}_1(r)$  and  $\bar{E}_2(\theta)$ , respectively. For larger  $N$ , the latest previously obtained set of converged coordinates is used as nominal parameters. Numerical calculations are performed on a CDC Cyber 170-series digital computer using default values of the IMSL convergence parameters.

Two measures of identification scheme performance are employed. The quantity

$$\hat{J}^{M,N} = \left( \frac{J^{M,N}}{L_r L_\theta} \right)^{1/2} \quad (38)$$

is used as a measure of state estimation accuracy. Additionally,

$$R^{M,N} = \frac{|E^{M,N} - \bar{E}|}{|\bar{E}|} \times 100\% \quad (39)$$

measures the relative error between the true

$$\bar{E}(r, \theta) = \bar{E}_1(r) \bar{E}_2(\theta) \quad (40)$$

and the estimated  $E(r, \theta)$  denoted by

$$E^{M,N}(r, \theta) = E_1^{M,N}(r) E_2^{M,N}(\theta) \quad (41)$$

which is calculated from (24) and (25) using the  $(M,N)^{th}$  level of state approximation obtained at step 8 of the computational procedure. In (39),  $|\cdot|$  denotes the  $L_2$  norm on  $[\epsilon, R] \times [0, 2\pi]$ .  $R^{M,N}$  provides a measure of parameter estimation accuracy.

Convergence in the sense that

$$R^{M,N} \rightarrow 0$$

and

$$\hat{J}^{M,N} \rightarrow 0$$

as

$$(M,N) \rightarrow \infty$$

depends on the ability of the cubic spline approximates (24) and (25) to accurately represent  $\bar{E}_1(r)$  and  $\bar{E}_2(\theta)$ . An exact pointwise fit can be obtained for  $\bar{E}_2(\theta)$  by choice of the 4  $\delta$ -coefficients in (25). However,  $\bar{E}_1(r)$  can at best be approximated to

$$\frac{|E_1(r) - \bar{E}_1(r)|}{|\bar{E}_1(r)|} = 1.23\%$$

relative error by (24) and (27) with  $M_1 = 4$ . Consequently, entries in the  $(R^{M,N}, \hat{J}^{M,N})$  sequence can be expected to cease decreasing past some  $(M,N)$  value. Less realistic examples in which (24) and (25) exactly fit simpler

( - 4 )

$\bar{E}_1(r)$  and  $\bar{E}_2(\theta)$  functions, and  $\hat{J}^{M,N}$  and  $R^{M,N}$  monotonically decrease with increasing  $(M,N)$  can be found in [15]. Also, using the best cubic spline fits to  $\bar{E}_1(r)$  and  $\bar{E}_2(\theta)$  obtained from (24) and (25) to define  $E(r,\theta)$ , along with the exact  $f(r,\theta)$  data, we observed that

$$\hat{J}^{M,N} = 0.087$$

uniformly in  $(M,N)$ . The following numerical results show that the parameter estimates from the identification procedure tend to improve (reduce) this  $\hat{J}^{M,N}$  value at the expense of  $R^{M,N}$ .

Example 1: Estimate  $E_2(\theta)$  holding  $E_1(r)$  fixed at the best cubic spline estimate of  $\bar{E}_1(r)$  using (24). Nominal parameters for the  $N = 4$  starting value are obtained by fitting (25) to

$$E_2^0(\theta) = 1 + \frac{1}{2} \cos \theta .$$

Four  $\delta$ -parameters are estimated and results summarized below.

N	$\hat{J}^{M,N}$ , m	$R^{M,N}$ , z	CP time, sec
4	0.0390	5.13	8
6	0.0384	5.57	23
8	0.0322	5.69	86
10	0.0347	6.01	105
12	0.0330	5.83	132

Essentially no improvement in state estimate was obtained past  $N = 8$ . The  $E_2^{M,N}(\theta)$  tended to 3.591 instead of  $\bar{E}_2(\theta) \equiv 3.391$ . The  $\approx 0.20$  bias is attributed to the inability of (24) to exactly fit  $\bar{E}_1(r)$ .

Example 2: Estimate  $E_1(r)$  holding  $E_2(\theta)$  fixed at the best cubic spline estimate of  $\bar{E}_2(\theta)$  using (25). Nominal parameters for the  $N = 4$  starting value are obtained by fitting (24) to

$$E_1^0(r) \equiv 1$$

Four parameters are estimated and results summarized below.

N	$\hat{J}^{M,N}, m$	$R^{M,N}, z$	CP time, sec
4	0.0355	32.25	22
6	0.0343	24.5	41
8	0.0270	4.39	75
10	0.0293	13.17	103
12	0.0275	8.08	130
14	0.0273	7.44	168
16	0.0271	7.59	222
18	0.0267	7.68	292
20	0.0264	8.03	370
22	0.0260	7.91	460
24	0.0267	8.11	578
26	0.0250	7.49	751
28	0.0203	7.58	847
30	0.0259	7.71	1050

From a state estimation viewpoint,  $N = 28$  provides the best accuracy. Overall, considering state, parameter and ease of computation,  $N = 8$  is best. Figure 3 shows the character of  $E_1^{M,N}(r)$  for selected values of  $N$ .

Example 3: Estimate both  $E_1(r)$  and  $E_2(\theta)$ . Nominal parameters are obtained as before for  $N = 4$  from

$$E_1^0(r) \equiv 5$$

$$E_2^0(\theta) = 1 - \frac{1}{4} \sin \theta$$

For each  $N$ , the first coefficient,  $\delta_1$ , is held fixed at its initial value. Seven parameters are estimated.

$N$	$\hat{J}^{M,N}, m$	$\hat{R}^{M,N}, z$	CP time, sec
4	0.0356	32.24	40
6	0.0341	28.71	67
8	0.0270	4.42	168
10	0.0293	13.18	209
12	0.0275	8.09	256
14	0.0273	7.45	337
16	0.0271	7.59	411
18	0.0267	7.69	490
20	0.0264	8.04	567
22	0.0262	7.90	651
24	0.0260	8.12	768
26	0.0260	7.47	945

Again, from overall considerations,  $N = 8$  gives the best results.



## VII. CONCLUDING REMARKS

In all examples we have been able to successfully estimate the surface shape of the model antenna. Similar results have been obtained where random noise (approximately 5% noise level) has been added to the data. These and other findings may be found in Section VI of [15].

## ACKNOWLEDGMENTS

Research reported here was supported in part by NASA Grant NAG-1-258 for the first and second authors, in part by NSF Grant MCS-8205355 and in part by AFOSR Grant 81-0198 for the first author, and NSF Grant MCS-8200883 for the second author. Parts of the efforts reported were carried out while the first two authors were in residence at the Institute for Computer Applications in Science and Engineering, NASA Langley Research Center, Hampton, VA, which is operated under NASA Contracts No. NAS1-15810 and No. NAS1-16394.

## REFERENCES

- [1] Banks, H. T., "Algorithms for Estimation in Distributed Models With Applications to Large Space Structures." Proc. Workshop on Applications of Distributed System Theory to the Control of Large Space Structures, JPL-Calif. Inst. Tech., Pasadena, CA, July 14-16, 1982.
- [2] Banks, H. T., and Crowley, J. M., "Parameter Estimation in Timoshenko Beam Models," Lefschetz Center for Dynamical Systems Report No. 82-14, Brown University, Providence, RI, June 1982; J. Astr. Sci., Vol. 31, pp. 381-397, 1983.
- [3] Banks, H. T., Crowley, J. M., and Kunisch, K., "Cubic Spline Approximation Techniques for Parameter Estimation in Distributed Systems," IEEE Trans. Auto. Control, Vol. AC-28, No. 7, pp. 773-786, July 1983.
- [4] Banks, H. T., and Daniel, P. L., "Parameter Estimation of Nonlinear Nonautonomous Distributed Systems," Proc. 20th IEEE Conf. on Decision and Control, San Diego, CA, pp. 228-232, 1981.
- [5] Banks, H. T., and Kunisch, K., "An Approximation Theory for Nonlinear Partial Differential Equations With Applications to Identification and Control," Lefschetz Center for Dynamical Systems Rept. 81-7, Brown University, Providence, RI, 1981; SIAM J. Control and Optimization, Vol. 20, pp. 815-849, 1982.

- [6] Banks, H. T., and Daniel, P. L., "Estimation of Variable Coefficients in Parabolic Distributed Systems," LCDS Rept. #82-22, Sept. 1982, Brown University, IEEE Trans. Auto. Control, to appear.
- [7] Russell, R. A., Campbell, T. G., and Freeland, R. E., "A Technology Development Program for Large Space Antennas," Paper No. IAF-80A33, Presented at Thirty-First International Astronautical Congress of the International Astronautical Federation, Tokyo, Japan, Sept. 21-28, 1980.
- [8] Sullivan, M. R., "LSST (Hoop/Column) Maypole Antenna Development Program," Parts I and II, NASA CR-3558, June 1982.
- [9] Banks, H. T., and Majda, G., "Modeling of Flexible Surfaces: A Preliminary Study," ICASE Rept. No. 83-19, Hampton, VA, May 1983; J. Math Modeling, to appear.
- [10] Sagan, H., Boundary and Eigenvalue Problems in Mathematical Physics, John Wiley & Sons, Inc., 1966.
- [11] Banks, H. T., "Distributed System Optimal Control and Parameter Estimation: Computational Techniques Using Spline Approximations," Lefschetz Center for Dynamical Systems Rept. 82-6, Brown University, Providence, RI, 1982; in Proc. 3rd IFAC Symposium on Control of Distributed Parameter Systems, Toulouse, France, S.P. 21-S.P. 27, June 29-July 2, 1982.
- [12] Banks, H. T., "A Survey of Some Problems and Recent Results for Parameter Estimation and Optimal Control in Delay and Distributed Parameter Systems," In Volterra and Functional Differential Equations (K. B. Hannsgen, et al., eds.), Marcel Dekker, New York, pp. 3-24, 1982.
- [13] Strang, G., and Fix, G. J., An Analysis of the Finite Element Method, Prentice-Hall, Inc., 1973.
- [14] Schultz, M. H., Spline Analysis, Prentice-Hall, Englewood Cliffs, NJ, 1973.
- [15] Banks, H. T., Daniel, P. L., and Armstrong, E. S., "A Spline-Based Parameter and State Estimation Technique for Static Models of Elastic Surfaces," ICASE Rept. No. 83-25, Hampton, VA, June 1983.
- [16] Bartels, R. H., and Stewart, G. W., "Algorithm 432 - A Solution of the Matrix Equation  $AX + XB = C$ ," Commun. ACM, Vol. 15, pp. 820-826, Sept. 1972.
- [17] More, J. J., "The Levenberg-Marquardt Algorithm," Implementation and Theory in Numerical Analysis (G. A. Watson, ed.), Lecture Notes in Mathematics 630, Springer-Verlag, 1977.

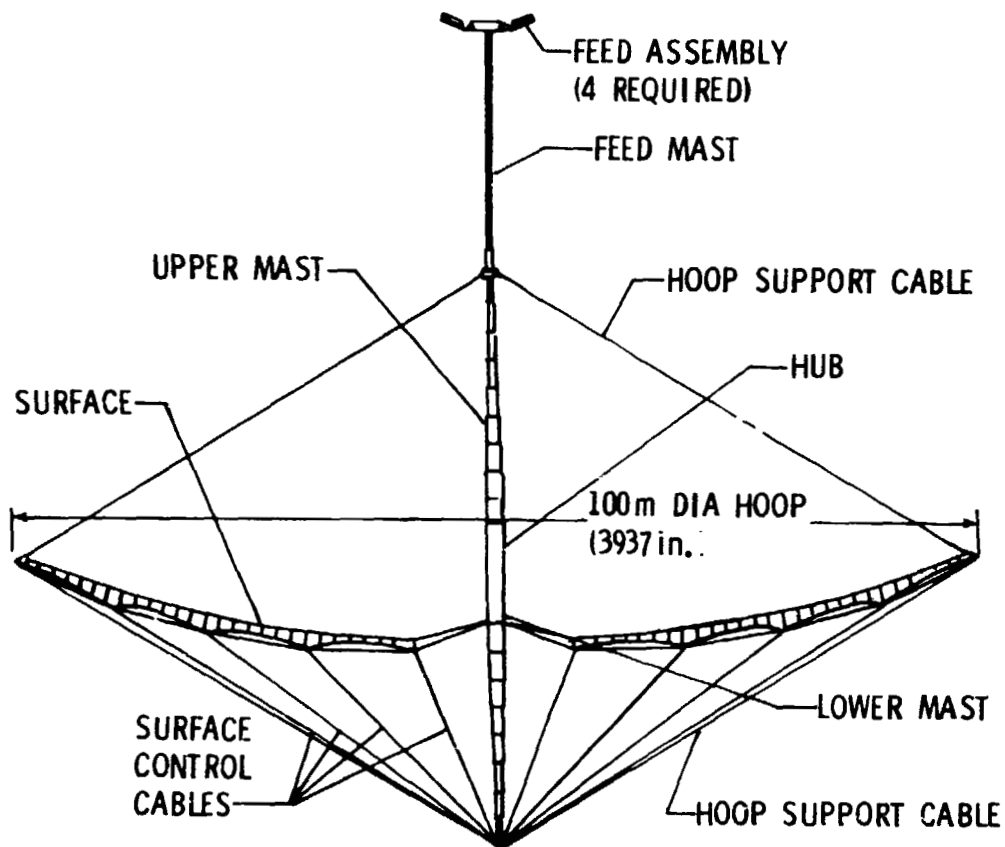


Figure 1.- Side View of Maypole (Hoop/Column) Antenna.

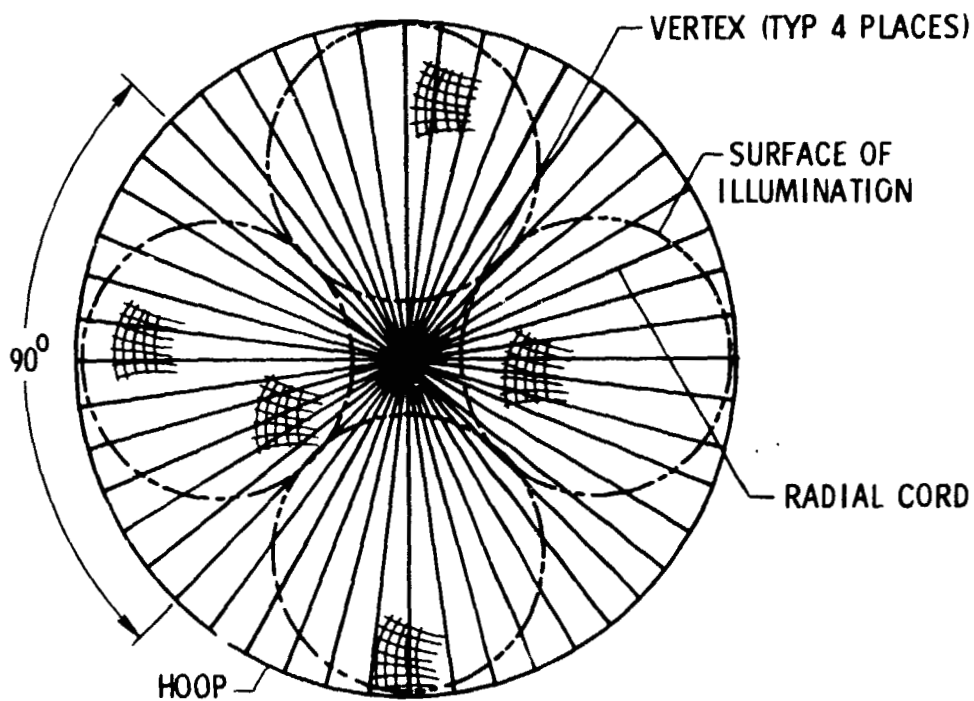


Figure 2.- Maypole (Hoop/Column) Antenna Reflector Surface.

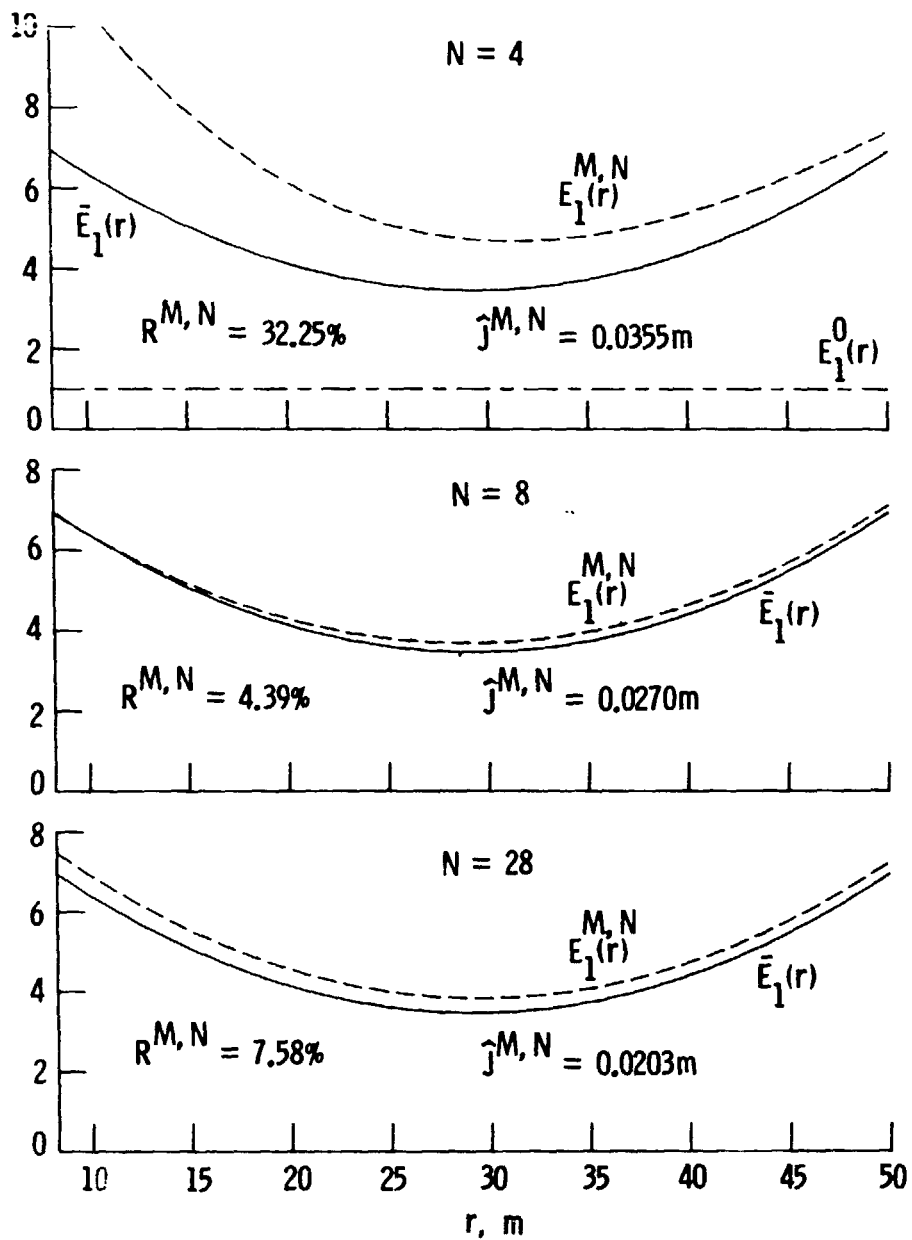


Figure 3.- Estimate  $E_1(r)$  with  $E_2(\theta)$  fixed.